IVYSPRING INTERNATIONAL PUBLISHER

Theranostics

2020; 10(21): 9789-9807. doi: 10.7150/thno.42508

Research Paper

Low-intensity Pulsed Ultrasound regulates alveolar bone homeostasis in experimental Periodontitis by diminishing Oxidative Stress

Siqi Ying[1,2,3], Minmin Tan[1,2,3], Ge Feng[1,2,3], Yunchun Kuang[1,2,3], Duanjing Chen[1,2,3], Jie Li[1,2,3]✉ and Jinlin Song[1,2,3]✉

1. College of Stomatology, Chongqing Medical University, Chongqing, China.
2. Chongqing Key Laboratory of Oral Diseases and Biomedical Sciences, Chongqing, China.
3. Chongqing Municipal Key Laboratory of Oral Biomedical Engineering of Higher Education, Chongqing, China.

✉ Corresponding authors: Dr. Jinlin Song, College of Stomatology, Chongqing Medical University. 426# Songshibei Road, Yubei District, Chongqing 401147, P.R. China. Tel.: +86-23-8886-0026; Fax: +86-23-8886-0222; E-mail address: songjinlin@hospital.cqmu.edu.cn, or; Dr. Jie Li, College of Stomatology, Chongqing Medical University. 426# Songshibei Road, Yubei District, Chongqing 401147, P.R. China. Tel.: +86-23-8860-2351; Fax: +86-23-8886-0222; E-mail address: jieli@hospital.cqmu.edu.cn.

Received: 2019.11.27; Accepted: 2020.07.28; Published: 2020.08.01

Abstract

Periodontitis is a widespread oral disease that results in the loss of alveolar bone. Low-intensity pulsed ultrasound (LIPUS), which is a new therapeutic option, promotes alveolar bone regeneration in periodontal bone injury models. This study investigated the protective effect of LIPUS on oxidative stress in periodontitis and the mechanism underlying this process.

Methods: An experimental periodontitis model was induced by administering a ligature. Immunohistochemistry was performed to detect the expression levels of oxidative stress, osteogenic, and osteoclastogenic markers *in vivo*. Cell viability and osteogenic differentiation were analyzed using the Cell Counting Kit-8, alkaline phosphatase, and Alizarin Red staining assays. A reactive oxygen species assay kit, lipid peroxidation MDA assay kit, and western blotting were used to determine oxidative stress status *in vitro*. To verify the role of nuclear factor erythroid 2-related factor 2 (Nrf2), an oxidative regulator, during LIPUS treatment, the siRNA technique and $Nrf2^{-/-}$ mice were used. The PI3K/Akt inhibitor LY294002 was utilized to identify the effects of the PI3K-Akt/Nrf2 signaling pathway.

Results: Alveolar bone resorption, which was experimentally induced by periodontitis *in vivo*, was alleviated by LIPUS via activation of Nrf2. Oxidative stress, induced via H_2O_2 treatment *in vitro*, inhibited cell viability and suppressed osteogenic differentiation. These effects were also alleviated by LIPUS treatment via Nrf2 activation. Nrf2 silencing blocked the antioxidant effect of LIPUS by diminishing heme oxygenase-1 expression. $Nrf2^{-/-}$ mice were susceptible to ligature-induced periodontitis, and the protective effect of LIPUS on alveolar bone dysfunction was weaker in these mice. Activation of Nrf2 by LIPUS was accompanied by activation of the PI3K/Akt pathway. The oxidative defense function of LIPUS was inhibited by exposure to LY294002 *in vitro*.

Conclusions: These results demonstrated that LIPUS regulates alveolar bone homeostasis in periodontitis by attenuating oxidative stress via the regulation of PI3K-Akt/Nrf2 signaling. Thus, Nrf2 plays a pivotal role in the protective effect exerted by LIPUS against ligature-induced experimental periodontitis.

Key words: periodontitis, alveolar bone, oxidative stress

Introduction

Periodontitis is a widespread oral disease that affects almost half of the adult population worldwide [1]. Its initiation and progression is considered to be due to an imbalance between inflammatory and host

immune responses caused by periodontal bacteria [2]. Treatments currently available for periodontitis include mechanical debridement, anti-inflammatory medication and regenerative surgery [3]. However, due to unsatisfactory outcomes associated with the use of anti-inflammatory drugs, alternative supplemental therapies are being increasingly considered as treatments for periodontitis.

The therapeutic potential of physical stimulation as an effective treatment for periodontitis has been described [4, 5]. Low-intensity pulsed ultrasound (LIPUS) is a non-invasive ultrasound technique that transmits low frequency and low-intensity sound waves into tissues as acoustic pressure waves [6, 7]. Conversion of mechanical signals emanating from these pressure waves to biochemical responses results in downstream effects [8]. Multiple experiments have demonstrated that LIPUS modulates bone tissue regeneration and accelerates bone repair processes by upregulating bone specific genes and downregulating osteoclast differentiation [9, 10]. Our latest studies indicated that LIPUS promoted alveolar bone regeneration *in vivo* [11] and facilitated osteogenic differentiation *in vitro* [12]. However, the precise mechanism by which LIPUS exerts protective effects on periodontitis remains unclear, thereby limiting the clinical application of LIPUS.

Oxidative stress is defined as an imbalance between the excessive production of reactive oxygen species (ROS) and a relative deficiency of antioxidants [13]. Numerous studies have demonstrated that oxidative stress is one of the pathophysiological mechanisms underlying inflammation, as well as periodontitis [14-18]. It was further established that periodontitis may be initiated by increased oxidative damage [19]. A previous study conducted by us revealed that oxidative stress impedes osteogenic differentiation and decreases regenerative potential [20]. Therefore, it is evident that oxidative stress plays an essential role in the pathological process of periodontitis. Besides, exploring modalities that decrease oxidative stress may reveal new avenues that show potential as periodontal treatments. Nuclear factor erythroid 2-related factor 2 (Nrf2) is a redox-sensitive transcription factor that upregulates a battery of antioxidant genes that defend against oxidative stress [21]. It has been reported that Nrf2 deficiency may accelerate osteoclastogenesis and elevate the oxidative damage [22]. $Nrf2^{-/-}$ mice exhibited more bone loss compared to wild-type mice [23]. By contrast, activated Nrf2 protected periodontal tissue from oxidative stress, periodontitis, and alveolar bone destruction [24-26]. Most importantly, LIPUS induced cytoprotective effects by reducing oxidative stress [26]. Therefore, we hypothesized that LIPUS may be useful as a new supplemental therapy for periodontitis.

The objectives of the present study were to elucidate the mechanisms underlying LIPUS-mediated protection against periodontitis and to determine the association between the roles played by LIPUS, oxidative stress, and Nrf2 in the development of periodontitis-induced alveolar bone destruction.

Materials and Methods

LIPUS application instructions

The LIPUS exposure device, manufactured by National Engineering Research Center of Ultrasound Medicine (Chongqing Medical University, Chongqing, China), consisted of an array of 6 transducers (each with a diameter of 34.8 mm), which were specifically designed for use in a 6-well culture plate. The LIPUS exposure device contains a focused transducer, which was positioned at the maxillary first and second molars to direct the acoustic beam to the desired region.

The parameters of LIPUS used in the present study consisted of a 1.5 MHz ultrasound signal with a 200 ms burst sine wave, pulsed 1:4 (2 ms on and 8 ms off) with a repetition rate of 1.0 kHz, and an average spatial and temporal intensity of 30, 60, and 90 mW/cm^2. The percentage permeability of ultrasound through the ultrasonic coupling gel, as determined via an ultrasound power meter (UPM-DT-1 AV; Ohmic Instruments, Easton, MD, USA), was 63.56±2.02. Control groups were handled in the same way as treatment groups, except for the fact that the ultrasound generator was not switched on.

Animal and treatment schedule

Animals

All experiments in this study were conducted in accordance with the Declaration of Helsinki, ARRIVE guidelines, and National Institutes of Health Guide for the Care and Use of Laboratory Animals under protocols reviewed and approved by the Ethics Committee of the College of Stomatology, Chongqing Medical University. C57BL/6 mice and Sprague-Dawley (SD) rats were purchased from the Experimental Animal Center of Chongqing Medical University (Chongqing, China), while $Nrf2^{-/-}$ mice with a C57BL/6 background were donated by Professor Gangyi Yang at the second affiliated hospital of Chongqing Medical University. All animals were housed in a specific pathogen-free room at Chongqing Key Laboratory of Oral Diseases and Biomedical Sciences and received water and food *ad libitum* from the Animal Care Facility Service.

Group allocation

Twenty SD rats were randomly divided into 4 groups of 5 each. The study groups were as follows: Control (no treatment), Ligature (ligature-induced experimental periodontitis for 14 days), LIPUS-only (LIPUS treatment for 14 days) and Ligature + LIPUS (experimental periodontitis before LIPUS treatment for 14 days). In a separate study, $Nrf2^{-/-}$ and Wild-type (WT) C57BL/6 mice were divided into 5 groups of 5 each. The study groups were as follows: $Nrf2^{+/+}$ (WT with no treatment), $Nrf2^{-/-}$ Control ($Nrf2^{-/-}$ with no treatment), $Nrf2^{-/-}$ Ligature ($Nrf2^{-/-}$ with ligature-induced experimental periodontitis for 8 days), $Nrf2^{-/-}$ LIPUS-only ($Nrf2^{-/-}$ with LIPUS treatment for 8 days), $Nrf2^{-/-}$ Ligature + LIPUS ($Nrf2^{-/-}$ with experimental periodontitis and LIPUS treatment for 8 days).

Each animal in the LIPUS-only group was treated with LIPUS daily for 30 min. In the ligature group and ligature + LIPUS group, animals underwent insertion of the ligature. In the latter group only, animals were also treated with LIPUS daily for 30 min after insertion of the ligature, whereas control animals were handled identically but without the LIPUS stimulation (Figure 1A and Figure 8B).

Animal ligature-induced periodontitis model

Establishing and inducing the experimental periodontitis model was performed as previously described [27]. Briefly, a 5-0 silk ligature was inserted between the maxillary left first and second molars and knots were tied on both ends to secure the ligature. The ligatures were examined daily to ensure that they remained in place during the experimental period. Periodontal inflammation and bone loss in this model is initiated by massive local accumulation of bacteria on the ligature-treated molars [28]. The contralateral side of each mouse was left without ligature treatment. A second set of controls included mice that were not treated with ligatures on either side.

Micro-computed tomography

The upper jaws were dissected and scanned using a high-resolution CT system (Skyscan 1172; Skyscan, Aartselaar, Belgium). Three-dimensional reconstructions were generated using Amira software. Scans were performed using the following scanner settings: X-ray source voltage 70 kVp, current 114 μA, and power 8 W. CT scan (Scanco Medical AG) settings were high resolution, voxel size of 15 μm, slice thickness of 0.01 mm, and FOV/diameter of 30.7 mm, while an integration time of 250 ms micro-CT was used to assess the loss of alveolar bone. To qualify bone loss, the six-site total cementoenamel junction and alveolar bone crest (CEJ-ABC) distance for the ligature-treated side of each mouse was subtracted from the six-site total CEJ-ABC distance of the contralateral side (no ligature treatment) of the same mouse. Bone density measurements were taken in samples oriented using the Scanco Medical analysis software. The maxillae were oriented with the first molar CEJ parallel to each other in the sagittal and coronal planes. The crowns of the first, second, and third molars were visible in the axial plane. After orientation, a 40-slice volume set at a threshold of 75 was considered to be the region of interest for analysis. Analysis started at the slice in which furcation first appeared, proceeding apically. BV/TV percentage and Tb.Th. values were recorded and averaged for each group ($n \geq 3$/group for all micro-CT analyses).

Paraffin sections

Following micro-CT scans, specimens were decalcified in 10% EDTA for at least 1 month, and then blocked parallel to the long axis of the left first and second molar on the lingual margin in order to allow subsequent histologic sections to show the interproximal region between the two teeth. Specimens were then dehydrated and embedded in paraffin, and 4 μm sections were made.

Immunohistochemistry

Periodontal sections were blocked in 10% normal goat serum; incubated overnight with primary antibodies against 3-nitrotyrosine (3-NT) (1:200) (Abcam, Cambridge, UK), 8-Hydroxy-2'-deoxy-guanosine 8-OHdG (1:200) (Abcam), Nrf2 (1:300) (Abcam), and HO-1 (1:300) (Abcam), Interleukin (IL)−6 (1:200) (Bioss), tumor necrosis factor alpha TNF-α (1:100) (Bioss), receptor activator of NF-κB ligand RANKL (1:300) (Abcam), alkalinephosphatase ALP (1:300) (Abcam) and osteocalcin OCN (1:200) (Abcam) at 4 °C; and stained with HRP-conjugated secondary antibodies (ZSJQ-BIO, Beijing, China). Diamino-benzidine (DAB) was used as a substrate for color development. All slides were counterstained with hematoxylin. Images of histologically stained sections were obtained using a BX41 microscope (Olympus, Japan). The H-score method [29] was applied for calculating the staining score of each sample, which was to multiply the immunoreaction intensity (negative: 0, weak: 1, moderate: 2, strong: 3) by the staining extent score (0%-100%). According to the H-score, the stained samples were divided into four groups: negative (-; 0), weak (+; 0~1), moderate (++; 1~1.5), and strong (+++; 1.5~3). Samples with a negative or weak H-score were determined to be the low protein expression group, whereas those with a moderate or strong H-score were classified as the high protein expression group.

TRAP staining

The TRAP stain was conducted with a Leukocyte Acid Phosphatase kit (Nanjin jianchen Bioengineering Institute, Nanjing, China). The TRAP-positive cells were photographed and counted with the Olympus BX41 microscope.

MPO flow analysis

Gingival tissues were homogenized in a solution composed of 3% type I collagenase (Sigma-Aldrich, St. Louis, MO, USA) in 50 mM sodium phosphate buffer. After homogenization, cells were fixed, permeabilized, and stained intracellularly with Anti-Myeloperoxidase antibody (Abcam) for 60 min at 4 °C, and then incubated with Goat Anti-rabbit IgG/Alexa Fluor 488 antibody (Bioss, Beijing, China) for 60 min. At least 1×10^4 cells were analyzed per sample. Flow cytometry was performed on a BD Influx flow cytometer (BD Biosciences, San Jose, CA).

Cell and treatment schedule

Cell culture

Healthy volunteers aged from 10 to 20 years, with informed consent from guardians, donated their teeth for orthodontic extraction treatment. Isolation and culturing of periodontal ligament cells (PDLCs) were performed as previously described [23]. Briefly, periodontal ligament tissue was carefully scraped from the middle third of the root and digested with 3 mg/mL of type I collagenase (Sigma-Aldrich) dissolved in phosphate-buffered saline at 37 °C for 30 min. Following full digestion, the periodontal ligament tissue suspension was seeded in α-Minimum Essential Medium (α-MEM; Hyclone, Logan, UT, USA) supplemented with 10% fetal bovine serum (FBS; Gibco, USA), 100 U/mL of penicillin and 100 μg/mL of streptomycin. The culture was incubated at 37 °C in a humidified atmosphere with 95% air and 5% CO_2. The cell culture medium was changed every 3 days. PDLCs were passaged at a ratio of 1:3 when they reached approximately 80% confluence. Pooled cell samples from the 3rd passage were used for further treatment.

Cell treatment

In order to establish the cellular oxidative stress model, PDLCs were exposed to H_2O_2 (Sigma) for 6 h after reaching approximately 90% confluence and further incubated in culture medium for 8 h. PDLCs were pretreated with LIPUS 30 min prior to the addition of H_2O_2 to investigate its effect on oxidative stress. All experiments were performed in triplicate.

Cell viability and evaluation of cell proliferation

PDLC proliferation was evaluated using Cell Counting Kit-8 (Beyotime Biotechnology, Shanghai, China). The treated cell suspension (5×10^3 cells/well) was seeded on a 96-well plate for 48 h. Next, cells were treated with CCK-8 reagent (Beyotime) and incubated for 2 h at 37 °C. Absorbance at 450 nm was measured using a microplate reader (Perkin Elmer, USA). All experiments were repeated in triplicate.

Osteogenic differentiation of PDLCs

Osteogenic induction was applied to detect the osteogenic differentiation capacity of PDLCs induced by H_2O_2 in the presence or absence of LIPUS pre-treatment. Cells were seeded at a density of 1×10^5 cells per well in a 6-well culture plate and incubated. When the cells reached 80% confluency, the medium was replaced with stem osteogenic differentiation medium [a-MEM supplemented with 10% FBS, 50 μg/mL of ascorbic acid (Sigma), 5 mM L-glycero-phosphate (Sigma), and 100 nM dexamethasone (Sigma) for 7-21 days depending on the experiment.

Alkaline phosphatase (ALP) staining was determined using NBT/BCIP (Beyotime) according to the manufacturer's protocol after 7 days of osteogenic induction. ALP activity was evaluated using an AKP analysis kit (Nanjing Jiancheng Bioengineering Institute, China) after 7 days, according to the manufacturer's instructions.

Calcium accumulation was detected by fixing with 4% fixative solution (Solarbio Co., Ltd., Beijing, China) and staining with 0.2% Alizarin Red (Solarbio) after 21 days of osteogenic induction. To quantify mineralization, cells stained with Alizarin Red were destained with 10% cetylpyridinium chloride mono-hydrate (Solarbio), following which the extracted stain was transferred to a 96-well plate, and the absorbance at 405 nm was measured using a microplate reader (Perkin Elmer, USA).

Detection of oxidative stress

Intracellular ROS were detected using an ROS Assay Kit (Beyotime, China). Following H_2O_2 exposure for 6 h, cells in six-well plates were incubated with 1 mL of 0.1% DCFH-DA diluted in a-MEM at 37 °C for 20 min and washed thrice with a-MEM. Green fluorescence was examined under a fluorescence microscope. Three days following H_2O_2 exposure, PDLCs were collected and protein was extracted. Protein concentration was determined using a BCA protein assay kit (Beyotime). MDA activity was detected using a Lipid Peroxidation MDA Assay Kit (Beyotime) according to the manufacturer's protocol. MDA concentrations were expressed as mol/g protein.

Quantitative RT-PCR analysis

Total RNA was extracted from PDLCs in a six-well plate using RNAiso Plus (Takara, Beijing, China). Next, 500 ng of total RNA was used as the template to synthesize cDNA using 5 X PrimeScript RT Master Mix (Takara). For PCR amplification, a 10-μL reaction volume was used, comprising 5 μg of 2 X TB Green Fast qPCR Mix (Takara), 0.1 mM of each primer, 1 μL of fivefold diluted cDNA and diethyl pyrocarbonate water (Sangon Biotech). The reaction and detection were conducted using a CFX96 Real-Time PCR Detection System (Bio-Rad Laboratories, Inc., Hercules, CA, USA). The cycle threshold (Ct) values were collected and normalized to the level of glyceraldehyde-3-phosphate dehydrogenase (*GAPDH*), a housekeeping gene. The primer sequences used for runt-related transcription factor-2 *(Runx2)*, *ALP, Nrf2, HO-1,* and *GAPDH* were as follows: *ALP* (F) 5′-TAA GGACATCGCCTACCAGCTC-3′, (R) 5′-TCTTCCAG GTGTCAACGAGGT-3′, *OCN* (F) 5′-GAATAGACTCC GGCGCTACC-3′, (R) 5′-AGCTCGTCACAATTGGG GTT-3′, *RANKL* (F) 5′-AGGATGCAACATACTTT GGG-3′, (R) 5′-TTGGGGCCATGCCTCTTAGT-3′, *IL-6* (F)5′-5GCCCTTCAGGAACAGCTATG-3′, (R) 5′-CAG AATTGCCATTGCACAAC-3′, *TNF-a* (F)5′-TGATCG GTCCCAACAAGGA-3′, (R) 5′-TGCTTGGTGGTTTG CTACGA-3′, *Nrf2* (F) 5′-TCAGAAACCAGTGGATCT GCC-3′, (R) 5′-AAGTGACTGAAACGTAGCCGA-3′, *HO-1* (F) 5′-CTCCCAGGGCCATGAACTTT-3′, (R) 50-GGGAAGATGCCATAGGCTCC-3′, and *GAPDH* (F) 50-CTTTGGTATCGTGGAAGGACTC-3′, (R) 5′-GTAGAGGCAGGGATGATGTTCT-3′.

Western blotting analysis

The total protein content of the cells was isolated using RIPA lysis buffer (Beyotime) with 1 mM phenylmethanesulfonyl fluoride (PMSF; Beyotime), and protein concentration was measured using a BCA protein assay kit (Beyotime). For each protein sample, 30 μg was separated via sodium dodecyl sulfate–polyacrylamide gel electrophoresis (SDS-PAGE; Beyotime), followed by transfer to a polyvinylidene difluoride membrane (PVDF; Bio-Rad). After blocking with 5% nonfat milk, the membranes were incubated with primary antibodies against 3-NT (1:2000) (Abcam), 4-Hydroxynonenal (4-HNE) (1:500) (Abcam), Phospho-Nrf2 (1:5000) (Abcam), Nrf2 (1:1500) (Abcam), HO-1 (1:2000) (Abcam), Phospho-Akt (1:1000) (Cell Signaling Technology, MA, USA), Akt (1:1500) (Cell Signaling Technology), and GAPDH (1:1000) (ZenBio, Chengdu, China) overnight at 4 °C, followed by the respective secondary antibodies: horseradish peroxidase (HRP)-conjugated goat anti-rabbit IgG (1:3000) (ZenBio) or HRP-conjugated goat anti-mouse IgG (1:3000) (ZenBio). Bands were detected using electrochemiluminescence plus reagent (Bio-Rad, USA). Finally, the intensity of these bands was quantified using ImageJ software (Version 1.8.0; National Institutes of Health, USA).

RNA silencing

In order to knock down Nrf2 expression, 1×10^5 PDLCs were transfected with siRNA-Nrf2 and siRNA-Negative control (siRNA-NC), purchased from Sangon (Shanghai, China). Transient siRNA transfection was performed with Lipohigh reagent (Sangon) according to the manufacturer's instructions. Following 24 h of transfection, the cells were treated with LIPUS and H_2O_2. Transfection efficiency was confirmed via qPCR and western blotting.

Immunofluorescence

Cells were treated with LIPUS and H_2O_2 to induce the translocation of Nrf2 into the nucleus. Meanwhile, PDLCs were pretreated with LY294002, a PI3K/Akt inhibitor. Following 48 h of treatment, cells were fixed using 4% paraformaldehyde and blocked with goat serum for 1 h. Cells were then incubated overnight with Nrf2 antibodies (1:500) (Abcam), and subsequently with goat anti-rabbit antibodies (1:400) (Bioss, China) conjugated with Alexa Fluor 555 for 1 h, on the following day. Cells were stained with DAPI. Images were acquired using an Olympus microscope (Olympus).

Statistical analysis

An unpaired Student's *t*-test was used when two independent groups were analyzed. For multiple comparisons, analysis of variance (ANOVA) was performed (one-way or two-way ANOVA) with a Tukey's post hoc test. Data are expressed as mean ± standard error of the mean (SEM). *p*-values of <0.05 were considered statistically significant. Analyses were performed using GraphPad Prism software (version 6.0, USA).

Results

LIPUS alleviates ligature-induced alveolar bone destruction in periodontitis

To determine whether LIPUS protects against ligature-induced experimental periodontitis, rats were treated with or without LIPUS daily for 14 days (Figure 1A). The CEJ-ABC distance reflects the degree of bone resorption quantitatively. BV/TV and Tb.Th. were used for bone volume density. Bone resorption in the ligature group was increased compared with that of the control group. However, it was alleviated by LIPUS. There was no significant difference in

alveolar bone destruction between the LIPUS-only group and the control group (Figure 1B-C). In addition, the ligature group showed a significant decrease in BV/TV and Tb.Th. compared with those of the controls, whereas LIPUS treatment significantly increased the levels of BV/TV and Tb.Th. Additionally, no difference was observed in the LIPUS treatment only compared with the control (Figure 1D-E).

LIPUS alleviates ligature-induced oxidative stress via Nrf2 Pathway

Histochemical analyses of decalcified H&E-stained bone sections indicate the protective effect exerted by LIPUS on ligature-induced experimental periodontitis models (Figure 2A). To clarified osteoblast and osteoclast activity, we stained ALP and OCN as osteogenic markers as well as IL-6, TNF-α, RANKL, and TRAP$^+$ cells as osteoclastogenesis molecular markers. In the immunohistochemistry evaluation, ALP and OCN levels were significantly alleviated in the ligature group as compared to controls, with a marked increase in osteoblast activation after LIPUS treatment (Figure 2A, Figure S1 and Figure 3A). RANKL, IL-6, TNF-α, and TRAP staining was the complete opposite (Figure 2A and S1). This further corroborates the results by showing that LIPUS reduced alveolar bone destruction in experimental periodontitis models. To investigate whether oxidative stress played a role in ligature-induced experimental periodontitis and LIPUS protection, we evaluated oxidative stress biomarkers, such as 3-NT, 8-OHdG, and MPO. Immunohistochemistry staining showed that rats in the ligature group showed significantly elevated levels of 3-NT and 8-OHdG-positive cells, compared with those in the control, while the 3-NT and 8-OHdG levels were reduced following LIPUS treatment (Figure 2A and Figure S3B). Flow cytometry analysis revealed significantly increased MPO expression in ligature groups, and levels of MPO expression descended significantly in ligature + LIPUS groups (Figure 2B). However, no significant difference was observed between the levels of these biomarkers in the control and LIPUS groups. Furthermore, Nrf2 and HO-1 expression levels in each group were examined, and the results showed that ligatures induced an increase in the levels of Nrf2 and HO-1, whereas treatment with LIPUS further significantly increased the levels of Nrf2 and HO-1 expression (Figure 2A and Figure S3B).

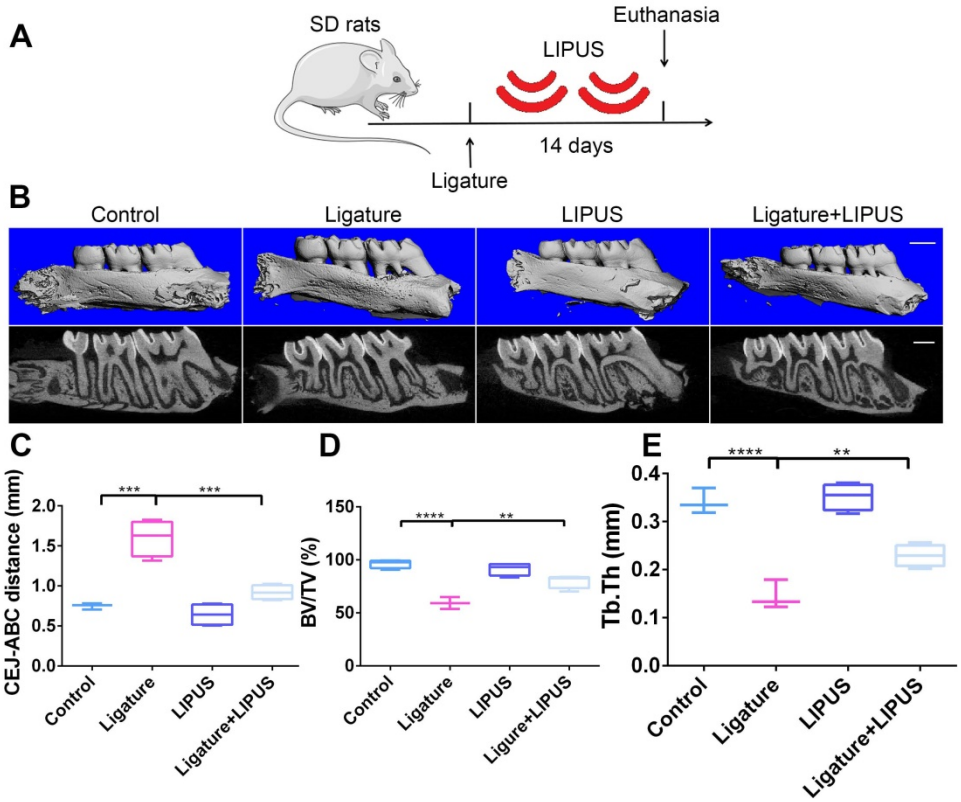

Figure 1. LIPUS alleviates ligature-induced alveolar bone destruction in periodontitis. (**A**) SD rats were subjected to subcutaneous ligature insertion for 14 d, with or without LIPUS treatment (30 min/day, with 200 ms pulses and 1.5 MHz) for 14 d. (**B**) Micro-CT image of the alveolar bone (Scale bar = 1 mm), (**C**) CEJ-ABC distance, (**D**) BV/TV, and (**E**) Tb.Th. Control (no treatment), Ligature (ligature-induced experimental periodontitis), LIPUS (only LIPUS treatment), Ligature + LIPUS (experimental periodontitis before LIPUS treatment). Data are presented as the mean ± SEM (n = 3). *, $p < 0.05$; **, $p < 0.005$; ***, $p < 0.0005$; ****, $p < 0.00005$.

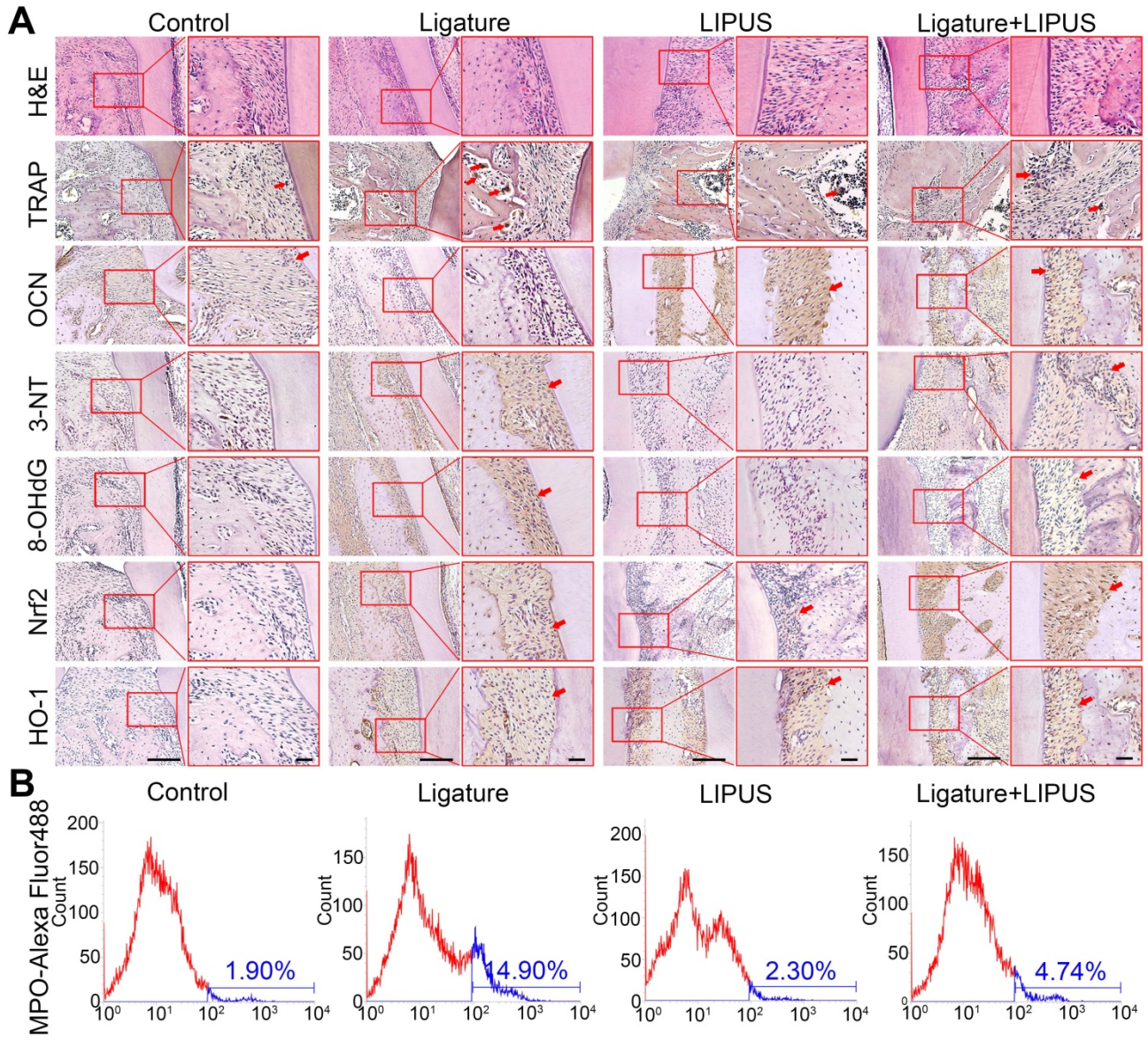

Figure 2. LIPUS alleviates ligature-induced oxidative stress via Nrf2 Pathway. (**A**) H&E staining at 200× and 400× magnification. TRAP staining, immunohistochemical staining of OCN, 3-NT, 8-OHdG, Nrf2, HO-1 at 200× and 400× (red box) magnification (Scale bar = 100 μm), (**B**) MPO flow analysis. Red arrows indicate positive staining.

H_2O_2 inhibits PDLC viability and osteogenesis

As a common ROS inducer, H_2O_2 was used in the following study to mimic oxidative stress in periodontitis. To determine a dosage of H_2O_2 that would be adequate to establish the cellular oxidative stress model, PDLCs were stimulated with diverse concentrations of H_2O_2, followed by measurement of cell viability. Compared with non-treated cells, cell viability was significantly reduced by 100 and 150 μM H_2O_2 ($p < 0.05$), 200 μM H_2O_2 ($p < 0.01$), and 250 μM H_2O_2 ($p < 0.005$). Accordingly, the H_2O_2 concentration that would be most suitable for use in subsequent experiments was ascertained to be 200 μM (Figure 3A). ALP staining in H_2O_2-exposed PDLCs was significantly decreased compared to staining at 0 h, in a time dependent manner (Figure 3B-C). The results suggest that induction by H_2O_2 for 6 h was adequate and this was applied in the subsequent studies.

LIPUS mitigates H_2O_2-induced inhibited cell viability and suppresses osteogenesis

The viability of PDLCs was measured in order to determine the effects of LIPUS on H_2O_2-induced suppression of cell viability and osteogenesis. A 30 min/day stimulation with LIPUS significantly enhanced cell viability compared with that of the other groups (Figure 4A). Simultaneously, cell viability, which was markedly lower than that of the control following H_2O_2-induction, was reversed by LIPUS treatment (Figure 4B). Therefore, the above results suggest that LIPUS rescued cell viability and promoted proliferation.

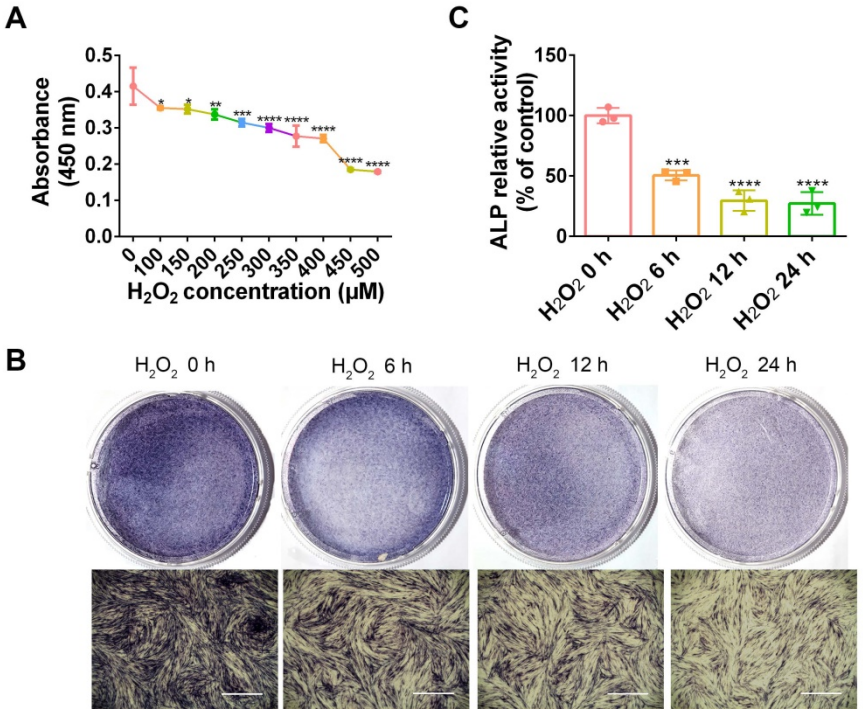

Figure 3. H2O2 inhibits cell viability and osteogenic differentiation. (**A**) Cell viability detected by the CCK-8 assay at different concentration of H2O2. Osteogenic differentiation at different exposure periods for H2O2 detected by ALP staining (Scale bar = 1 mm) (**B**) and ALP activity assay (**C**). Data are presented as the mean ± SEM (n = 3). *, $p < 0.05$; **, $p < 0.005$; ***, $p < 0.0005$; ****, $p < 0.00005$.

Next, to investigate the effects of LIPUS on both early and late stages of osteogenic differentiation in PDLCs, ALP and calcium were respectively evaluated. ALP and ARS (for calcium detection) staining results indicated that ALP and ARS in H_2O_2-exposed PDLCs, which were stained less compared to those of the control, were higher following LIPUS treatment (Figure 4C-E). We consistently observed that activity of ALP and calcium content in H_2O_2-exposed PDLCs were lower compared with those of the control, and that the levels of ALP activity and calcium content were attenuated by LIPUS treatment (Figure 4D-F). These data suggest that H_2O_2 inhibited both early as well as late stages of osteogenic differentiation in PDLCs, while LIPUS rescued the inhibitory effects of H_2O_2. Similarly, osteogenic differentiation and osteoclast differentiation were further evaluated via quantification of mRNA expression of the associated marker genes, *OCN*, *ALP*, *RANKL*, *IL-6*, and *TNF-α*. Both *OCN* and *ALP* were significantly downregulated following H_2O_2 induction, but upregulated following treatment with LIPUS (Figure 4G-H). *RANKL*, *IL-6*, and *TNF-α* stimulated by H_2O_2 were higher than those in the control, while those enhancements were inhibited by LIPUS treatment (Figure 4I-K).

LIPUS mitigates H_2O_2-induced oxidative stress

Oxidative stress has been reported to play a negative role in the progression of periodontitis [30]. To investigate whether LIPUS protects PDLCs against H_2O_2-induced oxidative stress, we performed an ROS activity assay and an MDA assay. The results showed that ROS accumulated in PDLCs after 6 h of treatment with H_2O_2, and that pretreatment with LIPUS decreased ROS accumulation induced by H_2O_2 (Figure 5A-C). Simultaneously, LIPUS suppressed H_2O_2-induced augmentation of MDA (Figure 5C), a biomarker of oxidative damage to lipids [31]. Additionally, H_2O_2 upregulated the protein expression of 3-NT and 4-HNE, biomarkers of oxidative damage [32], which were downregulated by LIPUS (Figure 5D-F).

LIPUS mitigates H_2O_2-induced oxidative stress via Nrf2 signaling pathway

Nrf2 is known to play a critical role in resisting oxidative stress by transcriptional activation of anti-oxidative enzymes such as HO-1, which reduce ROS and alleviate cell damage [33]. Nrf2 reportedly plays a pivotal role in oxidative responses [34]. Therefore, whether LIPUS alleviates oxidative stress by activating the Nrf2 signaling pathway was examined. The expression levels of *Nrf2* and *HO-1* among different groups were remarkably distinct (Figure 6A-B). LIPUS, by itself, did not increase Nrf2 and HO-1 gene expression. H_2O_2 alone did not affect the genetic expression level of Nrf2 until 9 h after H_2O_2 exposure, whereas the level of HO-1 increased immediately after H_2O_2 exposure. LIPUS

pretreatment significantly increased Nrf2 and HO-1 expression levels following exposure to H_2O_2, which remained high between 3 and 6 h. Therefore, the protein expression levels of Nrf2 and HO-1 were evaluated 6 h following exposure to H_2O_2. Western blotting results (Figure 6C-G) indicated that H_2O_2 exposure not only increased the activation of phospho-Nrf2 but also Nrf2 accumulation in the nucleus, which was further upregulated by LIPUS pretreatment. However, the expression of Nrf2 was not increased by exposure to H_2O_2.

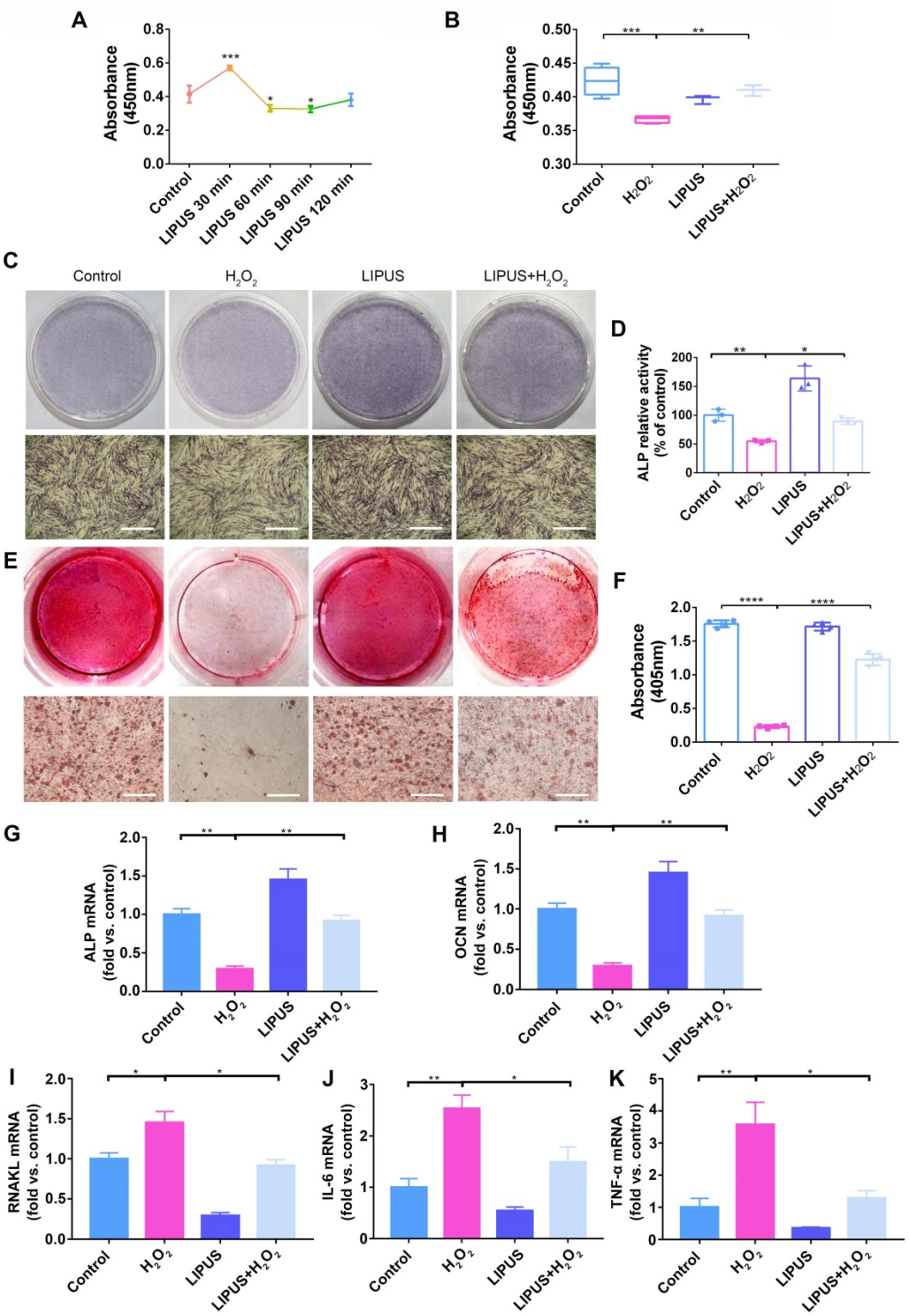

Figure 4. LIPUS mitigates H2O2-induced inhibited cell viability and suppressed osteogenesis. (**A**) Cell viability detected by the CCK-8 assay at different treatment periods for LIPUS. (**B**) Cell viability detected by the CCK-8 assay under H_2O_2 exposure and LIPUS treatment. Osteogenic differentiation detected by (**C**) ALP staining (Scale bar = 1 mm), (**D**) ALP activity, (**E**) Alizarin Red staining (Scale bar = 1 mm), (**F**) quantification of ARS staining, and gene expression of (**G**) *ALP*, (**H**) *OCN*, (**I**) *RANKL*, (**J**) *IL-6*, and (**K**) *TNF-α*. Data are presented as the mean ± SEM (n = 3). *, $p < 0.05$; **, $p < 0.005$; ***, $p < 0.0005$; ****, $p < 0.00005$.

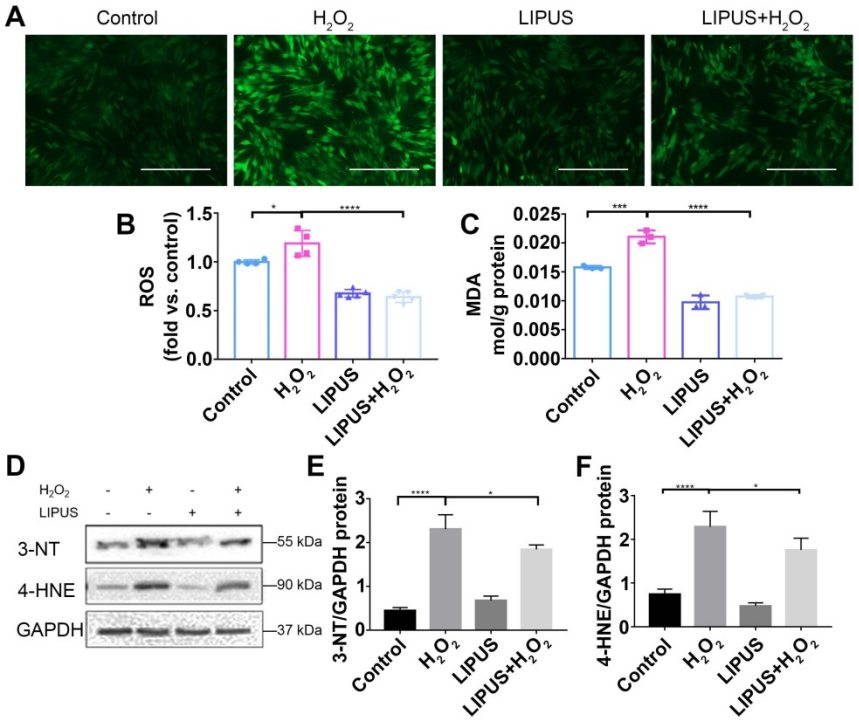

Figure 5. LIPUS mitigates H2O2-induced oxidative stress. Intracellular ROS measured by (**A**) DCFH-DA staining (Scale bar = 400 μm) and (**B**) DCFH-DA fluorescence intensity. (**C**) The MDA content of PDLCs was measured by MDA assay kit. Expression of 3-NT and 4-HNE were evaluated by (**D**) western blot. The representative expression of (**E**) 3-NT and (**F**) 4-HNE were measured by semi-quantitative analysis. Data are presented as the mean ± SEM (n = 3). *, $p < 0.05$; **, $p < 0.005$; ***, $p < 0.0005$; ****, $p < 0.00005$.

Knockdown of Nrf2 gene abrogates the protection of LIPUS against H_2O_2-induced oxidative stress

Application of siRNA knockdown was utilized to further determine distinct characteristics of Nrf2 that may be involved in the protection effect exerted by LIPUS on H_2O_2-induced oxidative stress. Transfection efficiency was confirmed by qPCR (Figure 7A) and western blotting (Figure 7B-C). Following exposure to H_2O_2, phospho-Nrf2 activation, HO-1 expression, and nuclear phospho-Nrf2 accumulation were upregulated compared with those of the negative control and further upregulated by LIPUS pretreatment. However, phospho-Nrf2 activation, HO-1 expression, and nuclear phospho-Nrf2 accumulation were decreased in the silenced group (Figure 7D-H). The above results indicate that LIPUS protects against H_2O_2-induced oxidative stress by activating the Nrf2 pathway.

Knockout of *Nrf2* weakens the protective effect exerted by LIPUS on ligature-induced alveolar bone destruction in periodontitis

In order to clarify the direct role of Nrf2 in LIPUS-mediated protection against periodontitis and bone resorption, ligature was applied to $Nrf2^{-/-}$ mouse models to induce experimental periodontitis following which the mice were treated with LIPUS for 8 days simultaneously. Next, gingival tissues were harvested as illustrated (Figure 8B). A western blot revealed minimal Nrf2 or HO-1 expression in $Nrf2^{-/-}$ mice (Figure 8A, C). These results indicated that deletion of *Nrf2* abolished the activation of Nrf2 and the expression of its antioxidant genes downstream. Compared with $Nrf2^{+/+}$ mice, ligature-treated $Nrf2^{-/-}$ mice showed a further decrease in bone resorption, where LIPUS did not rescue ligature-induced bone loss. Meanwhile, LIPUS-only treatment made no impact on destruction of alveolar bone (Figure 8D-G). Almost no Nrf2 expression was observed regardless of LIPUS treatment or experimental induction of periodontitis (Figure 8H-J). Interestingly, Nrf2 abrogation resulted in a moderate decrease of some antioxidants (HO-1). However, following LIPUS treatment, a significant upregulation of HO-1 was observed in $Nrf2^{-/-}$ mice (Figure 8H-J). Hence, it is surmised that LIPUS treatment did not reverse alveolar bone destruction in $Nrf2^{-/-}$ mice and that deletion of *Nrf2* may exacerbate HO-1 expression reactively. In addition, by the $Nrf2^{-/-}$ ligature group, the osteogenesis markers ALP and OCN were decreased as compared with that in the $Nrf2^{+/+}$ group and the $Nrf2^{-/-}$ control group, and ALP and OCN showed insignificant increases in the $Nrf2^{-/-}$ ligature + LIPUS group (Figure 9A and Figure S2). Significant induction of IL-6, TNF-α, RANKL, and TRAP staining was shown by histochemical detection in the $Nrf2^{-/-}$

ligature groups, and LIPUS treatment did not decrease osteoclastogenesis in the Nrf2$^{-/-}$ ligature + LIPUS groups (Figure 9A, Figure S2 and S3).

Knockout of *Nrf2* abolishes the protection of LIPUS against ligature-induced oxidative stress

The oxidative damage markers, 3-NT and 8-OHdG, were evaluated to investigate the effect of Nrf2 on LIPUS-mediated protection against ligature-induced oxidative stress in experimental periodontitis. Immunohistochemistry indicated almost no Nrf2 expression with or without LIPUS treatment in Nrf2$^{-/-}$ mouse experimental periodontitis models. Furthermore, significant HO-1 expression, observed in Nrf2$^{-/-}$ mice with experimental periodontitis, was further boosted due to LIPUS treatment, compared with that of Nrf2$^{+/+}$ mice (Figure 9A). Increased accumulation of 3-NT, 8-OHdG, and MPO was observed in Nrf2$^{-/-}$ mice in which the ligature significantly induced oxidative damage, compared with that of the Nrf2$^{-/-}$ control group and wild type. However, LIPUS treatment did not prevent these pathological changes in Nrf2$^{-/-}$ mice. Hence, the deletion of *Nrf2* exacerbated ligature-induced oxidative damage and inhibited the protective effect of LIPUS against ligature-induced oxidative damage (Figure 9A and 9B).

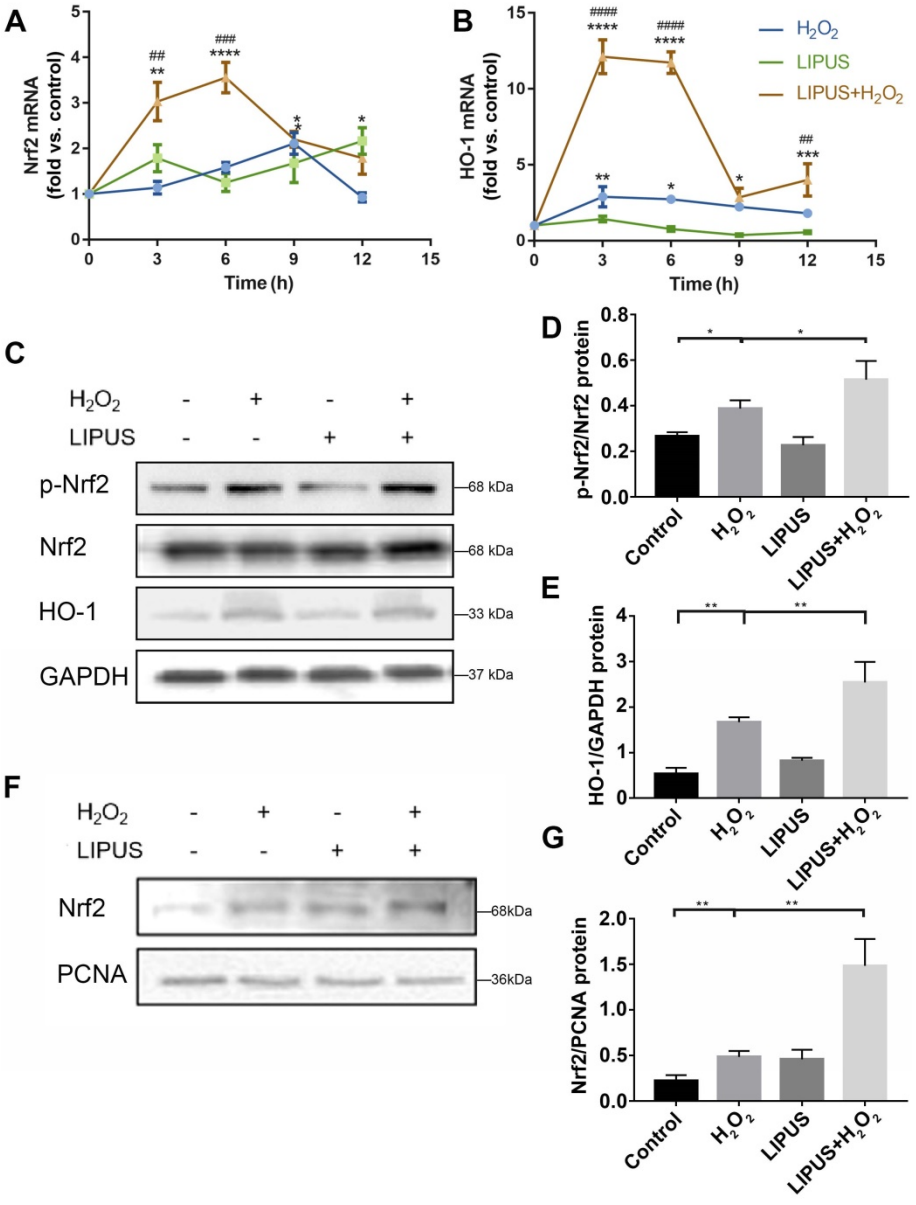

Figure 6. LIPUS mitigates H_2O_2-induced oxidative stress via Nrf2 signaling pathway. After H_2O_2-induced oxidative stress and LIPUS treatment, mRNA expression of (**A**) Nrf2 and (**B**) HO-1 was examined by qPCR. (**C**) Activation of phospho-Nrf2 and HO-1 were examined by western blot. The representative activation of (**D**) phospho-Nrf2 and (**E**) HO-1 were measured by semi-quantitative analysis. (**F**) Expression of Nrf2 in the nucleus was examined by western blot. (**G**) The quantitative expression of Nrf2 in the nucleus was measured by semi-quantitative analysis. Data are presented as the mean ± SEM (n = 3). *, $p < 0.05$; **, $p < 0.005$; ***, $p < 0.0005$; ****, $p < 0.00005$.

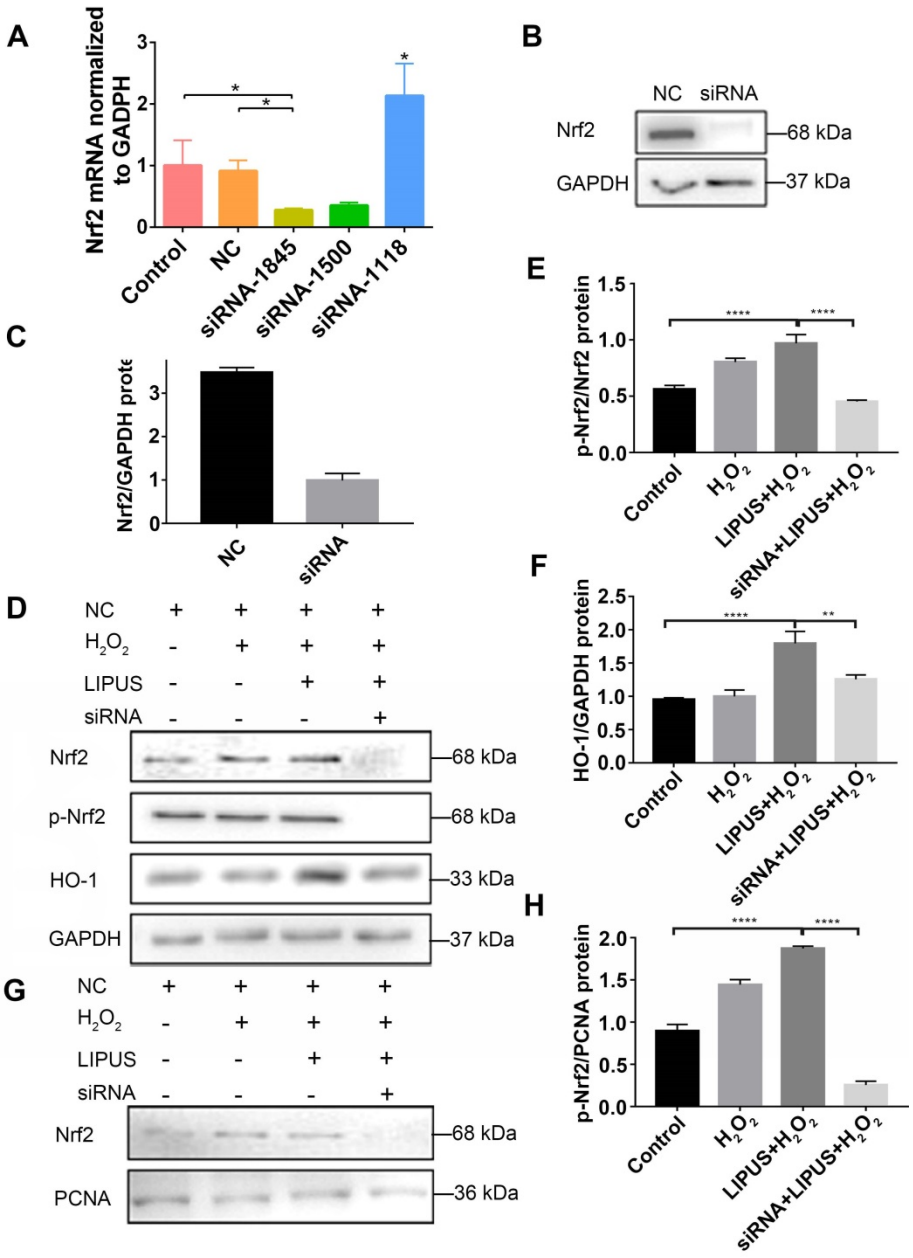

Figure 7. Knockdown of Nrf2 gene abrogates the protection of LIPUS against H_2O_2-induced oxidative stress. Transfection effects of small interfering RNA (siRNA) or negative control siRNA (NC) were analyzed by (**A**) qPCR and (**B**) western bloting. (**C**) The quantitative expression of Nrf2 in the nucleus was measured by semi-quantitative analysis. (**D**) After transfection with siRNA, activation of phospho-Nrf2 and HO-1 were examined by western blotting. The respective activation of (**E**) phospho-Nrf2 and (**F**) HO-1 were measured by semi-quantitative analysis. (**G**) Expression of Nrf2 in the nucleus was examined by western blot. (**H**) The quantitative expression of Nrf2 in the nucleus was measured by semi-quantitative analysis. Data are presented as the mean ± SEM (n = 3). *, $p < 0.05$; **, $p < 0.005$; ***, $p < 0.0005$; ****, $p < 0.00005$.

Inhibition of PI3K/Akt abrogated the protection of LIPUS against H_2O_2-induced oxidative stress

PI3K/Akt is a well-known upstream regulator of Nrf2 [35]. LY294002, an inhibitor of PI3K/Akt [35], was used to further confirm whether LIPUS acts against H_2O_2-induced oxidative stress via the PI3K/Akt pathway. Western blotting indicated that LIPUS pretreatment significantly increased the activation of phospho-Akt following H_2O_2 exposure (Figure 10A, D). However, LY294002 reversed the LIPUS-promoted activation of phospho-Akt and phospho-Nrf2, blocked the LIPUS-facilitated expression of HO-1, and inhibited the LIPUS-mediated up-regulation of nuclear Nrf2 (Figure 10B-C, E-H). Immunofluorescence analysis using anti-Nrf2 further confirmed these results by indicating that H_2O_2 enhanced Nrf2 accumulation in the nucleus, where LIPUS pretreatment further accelerated it. However, LY294002 reversed its translocation into the nucleus (Figure 10I). These results indicate that LIPUS exerted a protective effect against H_2O_2-induced oxidative stress via the PI3K-Akt/Nrf2 pathway.

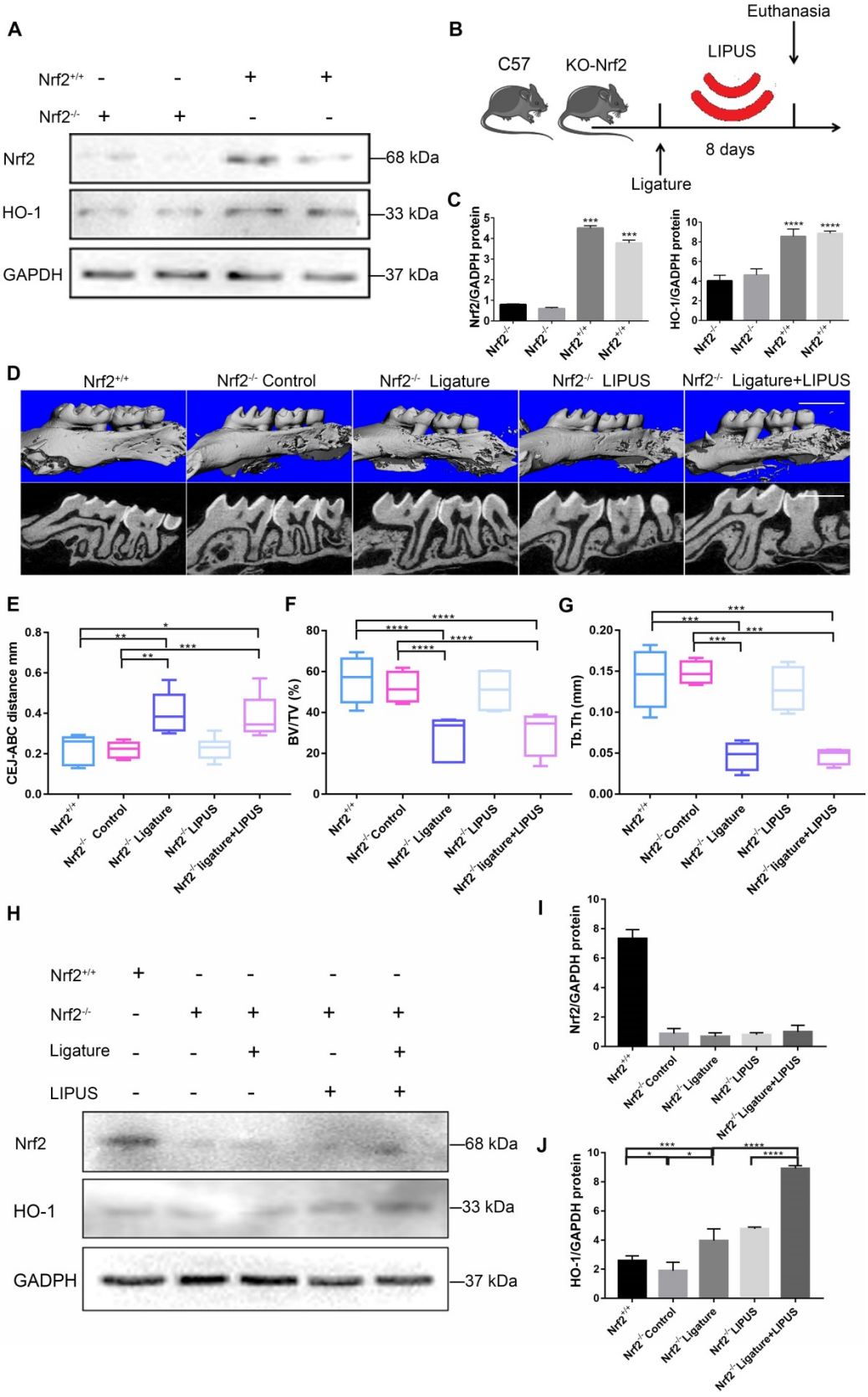

Figure 8. Knockout of *Nrf2* weakens the protection effect exerted by LIPUS on ligature-induced alveolar bone destruction in periodontitis. Nrf2$^{+/+}$ mice and Nrf2$^{-/-}$ mice were subjected to ligature insertion, with or without LIPUS treatment (30 min/day, with 200 ms pulses and 1.5 MHz) for 8 days simultaneously as described in Fig. 8B. Expression of Nrf2 and HO-1 was examined by western bloting. Activation of Nrf2 and HO-1 (**A**) quantitative levels (**C**). Three-dimensional image of the alveolar bone (Scale bar = 1 mm) (**D**). (**E**) CEJ-ABC distance, (**F**) BV/TV, and (**G**) Tb.Th. Nrf2 (**I**) and HO-1 (**J**) quantitative levels (**H**). Nrf2$^{+/+}$ (WT with no treatment), Nrf2$^{-/-}$ Control (Nrf2$^{-/-}$ with no treatment), Nrf2$^{-/-}$ Ligature (Nrf2$^{-/-}$ with ligature-induced experimental periodontitis), Nrf2$^{-/-}$ LIPUS (Nrf2$^{-/-}$ with LIPUS treatment only), Nrf2$^{-/-}$ Ligature+LIPUS (Nrf2$^{-/-}$ with experimental periodontitis and LIPUS treatment). Data are presented as the mean ± SEM (n = 3). *, $p < 0.05$; **, $p < 0.005$; ***, $p < 0.0005$; ****, $p < 0.00005$.

Discussion

Periodontitis is among the most widespread inflammatory diseases [1]. Multiple studies exploring the modalities in periodontitis treatment are being conducted [36]. Conventional efforts have focused on pathogen elimination [37], inflammation control [37], and immunity modulation [38]. However, current treatments have been found to be unsatisfactory, and the need for novel treatment options has been recognized. The current study applied LIPUS to manage alveolar bone homeostasis in periodontitis. Moreover, it was realized that reducing oxidative stress may provide a new perspective for future studies associated with periodontal treatment.

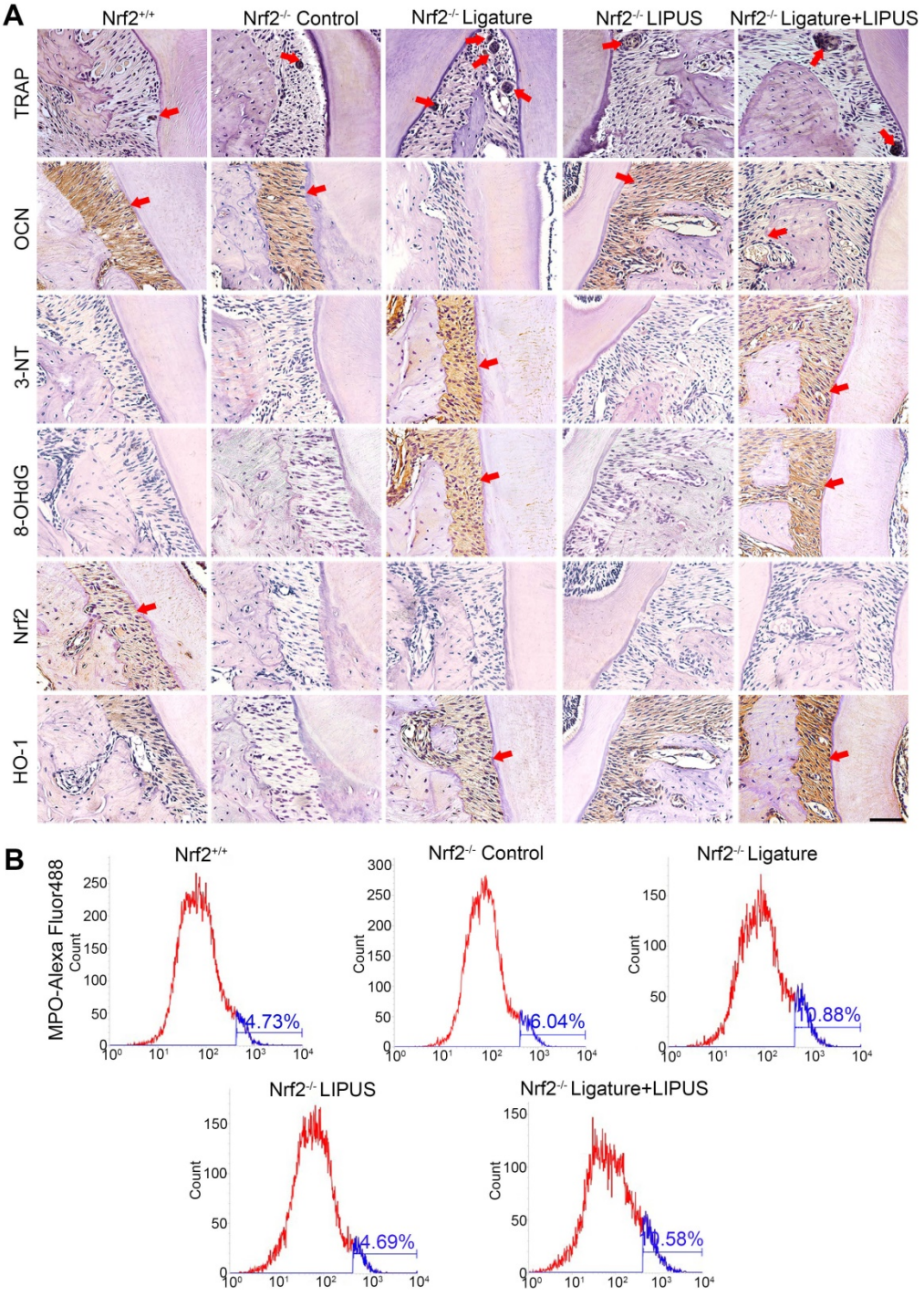

Figure 9. Knockout of *Nrf2* abolishes the protection of LIPUS against ligature-induced oxidative stress. (**A**) TRAP staining, immunohistochemical staining of OCN, 3-NT, 8-OHdG, Nrf2, and HO-1 at 400× magnification in periodontal tissue (Scale bar = 100 μm). (**B**) MPO flow analysis. Red arrows indicate positive staining.

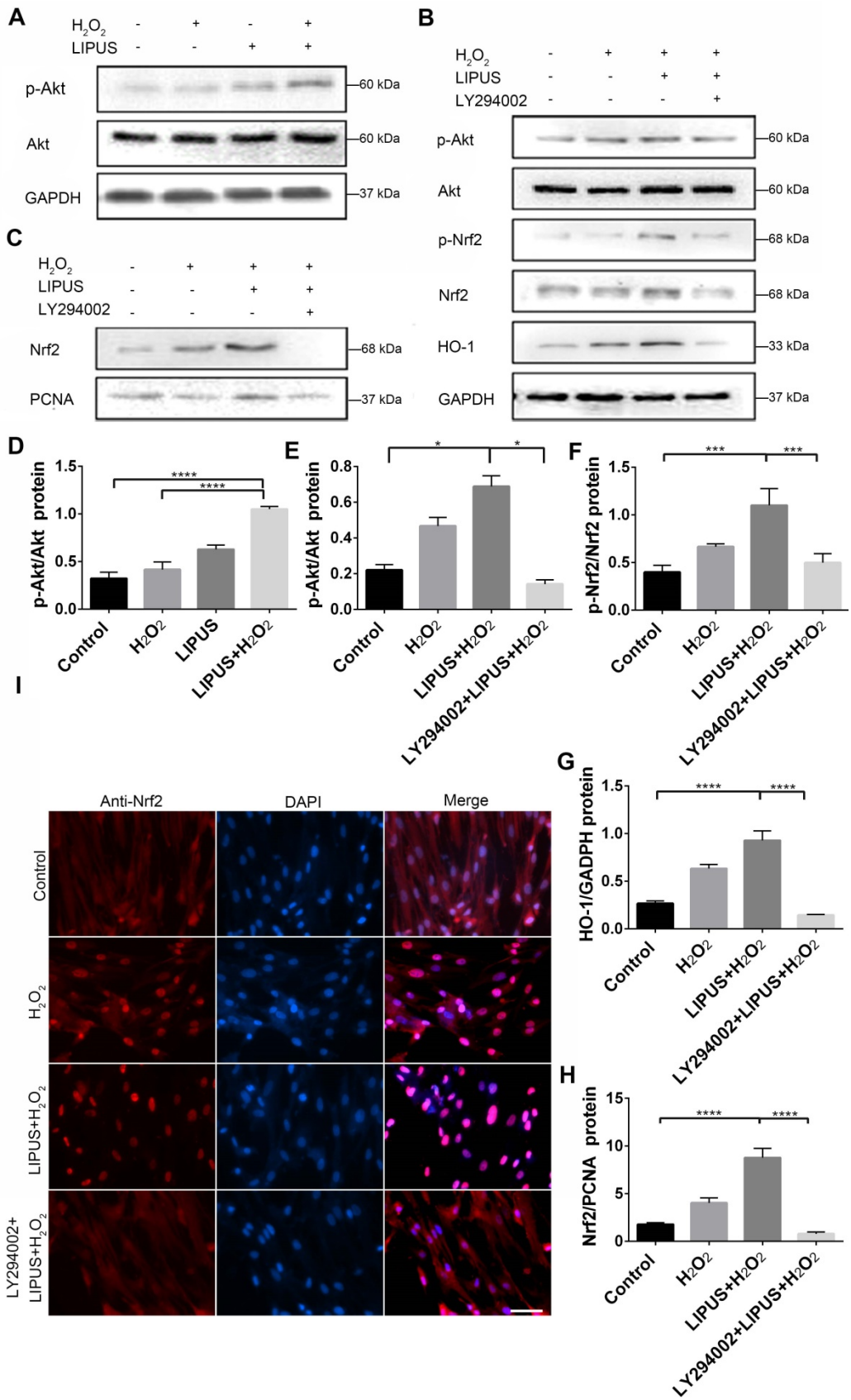

Figure 10. Inhibition of PI3K/Akt abrogated the protection of LIPUS against H_2O_2-induced oxidative stress. (**A**) Activation of phospho-Akt was examined by western blotting. (**D**) The quantitative activation of Nrf2 was measured by semi-quantitative analysis. (**B**) Pretreatment of LY294002 (10 μM), activation of phospho-Akt, phospho-Nrf2 and HO-1 were examined by western blotting. The respective activations of phospho-Akt (**E**), phospho-Nrf2 (**F**) and HO-1 (**G**) were measured by semi-quantitative analysis. (**C**) Expression of Nrf2 in the nucleus was examined by western blot. (**H**) The quantitative expression of Nrf2 in the nucleus was measured by semi-quantitative analysis. (**I**) Nrf2 translocation was determined by immunofluorescence at 200× magnification (Scale bar = 200 μm). Red: Nrf2-staining, blue: nucleus (DAPI), and pink: merger of blue and red indicating nuclear localization of Nrf2. Data are presented as the mean ± SEM (n = 3). *, $p < 0.05$; **, $p < 0.005$; ***, $p < 0.0005$; ****, $p < 0.00005$.

LIPUS is a clinically established, Food and Drug Administration (FDA)-approved therapy that is widely used to enhance bone growth during healing of non-union fractures and other osseous defects [39-41]. LIPUS induces mechanical stress stimulating osteogenesis via modulation of calcium ion channels [42, 43]. Previously, Li *et al*. first revealed that LIPUS may prevent bone loss due to osteoporosis [43]. Later, Yue *et al*. demonstrated that LIPUS enhanced osteogenesis of adipose stem cells by upregulating osteogenic genes [44]. Meanwhile, Carina *et al*. and Meng *et al*. implied that LIPUS treatment effectively impaired osteoclast differentiation and produced a reduction in osteoclast markers. Most importantly, our previous studies have shown that LIPUS exerts potential protective effects on alveolar bone regeneration in periodontal injury models [11] and facilitates osteogenic differentiation of PDLCs [12]. These results were confirmed by micro-CT imaging, CEJ-ABC distances, BV/TV, Tb.Th., and H&E staining, which revealed that LIPUS significantly attenuated ligature-induced alveolar bone loss (Figure 1). Histology staining also showed that LIPUS prevented alveolar bone loss, which was associated with increased osteoblast differentiation and low osteoclast activity. The above results clearly indicate that LIPUS exerts a protective effect on alveolar bone destruction in ligature-induced periodontitis. Also, many case-control studies have reported a direct link between periodontitis and oxidative stress [19, 45-47]. However, evidence indicating that oxidative stress plays a direct role in LIPUS protection is lacking. The findings of the current study led to the hypothesis that LIPUS moderate alveolar bone destruction in ligature-induced periodontitis via oxidative stress.

Oxidative stress is a redox state leading to excessive generation of ROS that causes severe damage to cells and tissues [48-50]. Periodontitis is a widespread oral disease which is associated with high ROS levels [51]. In previous clinical studies, high levels of ROS have been found to be elevated in the periodontal tissue of patients with periodontitis [52]. Heightened oxidative stress in periodontal tissues results in the release of large amounts of ROS [53]. Increased intracellular ROS levels were shown to support osteoclast differentiation and subsequent bone resorption [54]. Meanwhile, the oxidative stress-induced lower activity of antioxidant enzymes suppressed osteogenic differentiation and aggravated the pathological process of periodontitis [19]. Additionally, proteins and genes are major targets of oxidative damage [55]. 3-NT represents a commonly used biomarker for protein oxidation [56], and 8-OHdG represents the most widely accepted assay for DNA oxidative damage [57]. The present study confirms that ligatures induced oxidative damage by significantly increasing 3-NT and 8-OHdG in our experiment periodontal models, both of which were reversed by LIPUS. These results implied that LIPUS mitigated alveolar bone resorption in periodontitis by downregulating oxidative stress.

These observations prompted us to consider whether LIPUS facilitates osteogenic differentiation in PDLCs by reducing oxidative stress. H_2O_2 acts similarly to ROS, which permeate through cell membranes to initiate oxidative stress [58]. Numerous reports have indicated that H_2O_2 may be used to establish an *in vitro* oxidative stress model [59-61]. As indicated by the current study, following exposure to 200 μM H_2O_2 for 6 h, PDLCs displayed inhibited cell viability, suppressed osteogenic differentiation, and promoted osteoclast activity. However, LIPUS exerted cytoprotective activity by recovering cell viability and promoting osteogenic differentiation in H_2O_2-exposed cells. Intracellular ROS has been reported to be an indicator that directly reflects oxidative stress levels [61-63]. Oxidative stress is a consequence of an increase in oxidizing species or a decrease in anti-oxidant levels [64]. The extent of oxidative stress may be indicated by MDA as well. The present study demonstrates that the levels of ROS and MDA were significantly increased following H_2O_2 exposure but were reversed by LIPUS treatment. Additionally, oxidative stress also led to lipid peroxidation and resulted in 4-HNE production [65]. The present results show that the high expression levels of 3-NT and 4-HNE caused by H_2O_2 exposure were over-turned by LIPUS in PDLCs. Therefore, these results reveal that LIPUS significantly attenuated H_2O_2-induced oxidative stress, inhibition of cell viability, and suppression of osteogenic differentiation. Considered together, the results of the present study indicate that LIPUS alleviates osteogenesis differentiation in periodontal tissue by downregulating oxidative stress.

Nrf2, a master regulator of cellular redox homeostasis, activates cellular defense against oxidative stress by inducing hundreds of antioxidant and detoxifying enzymes [66, 67]. Cytoplasmic Nrf2, which is released from the Keap1-Nrf2 complex in response to oxidative stress, binds to antioxidant response elements in the promoter region of many genes encoding antioxidant enzymes [67]. Up-regulation of antioxidant enzymes, most of which are regulated by Nrf2, has been shown to inhibit oxidative stress [68]. The expression of Nrf2 and the downstream antioxidant enzyme, HO-1, were increased in ligature-induced alveolar bone destruction. Besides, Nrf2 expression and its function were further upregulated following LIPUS treatment.

Based on these findings, we surmised that LIPUS-associated protection may be strongly linked to Nrf2-mediated antioxidant defense mechanisms. Following its detachment from the Keap1-Nrf2 complex due to anti-oxidative stress, phospho-Nrf2 is activated and translocated to the nucleus and causes induction of antioxidant gene transcription [69, 70]. Therefore, western blot and qPCR were utilized to examine the activation of phospho-Nrf2, its nuclear translocation, and transcription of cytoprotective genes. The results indicate that LIPUS activated phospho-Nrf2, increased Nrf2 in the nucleus, and upregulated HO-1 expression. Previous studies have revealed that disruption of Nrf2 leads to increased oxidative stress and suppression of antioxidant capacity [71]. Furthermore, silencing Nrf2 expression significantly suppressed antioxidant capacity in PDLCs regardless of LIPUS treatment. LIPUS did not significantly alleviate ligature-induced promotion of osteogenic differentiation and suppression of osteoblast activity, which leads to an increase in bone resorption in Nrf2-deficient mice. LIPUS had no effects on ligature-induced oxidative damage in $Nrf2^{-/-}$ mouse models. These results clarify the pivotal role played by Nrf2-mediated antioxidant defense mechanisms *in vitro* and *in vivo*, and indicated that LIPUS alleviates oxidative stress and alveolar bone resorption via Nrf2 activation in periodontitis.

Upregulation of Nrf2 in PDLCs by LIPUS required further clarification. PI3K/Akt is a well-known upstream regulator of Nrf2 and activation of PI3K/AKT directly decreases Nrf2 degradation by promoting Nrf2 phosphorylation and accelerating its translocation into nuclei [26, 72]. Decreased Nrf2 degradation may initiate the transcription of downstream antioxidant genes that defend against oxidative stress [71]. Coincidentally, several past studies have indicated that LIPUS activated the PI3K/AKT pathway, thereby promoting its function [26, 73]. In order to elucidate the mechanism underlying the above process, we examined whether PI3K/Akt is mediated by LIPUS via upregulation of Nrf2 expression. Western blot and immuno-fluorescence showed that LIPUS upregulated the activation of phospho-Nrf2 and its accumulation in the nucleus, in an oxidative stress micro-environment. To investigate the role of the PI3K/Akt pathway further, LY294002, a pharmacological inhibitor of the PI3K/Akt pathway, was used. Inhibition of the PI3K/Akt signaling pathway markedly blocked Nrf2 and its downstream antioxidant expression, which confirmed that the PI3K-AKT pathway facilitates the regulation of Nrf2 by LIPUS under oxidative stress. These results suggest that LIPUS alleviated alveolar bone destruction in periodontitis by diminishing oxidative stress, and that this process was partially facilitated by PI3K-Akt/Nrf2 signaling.

Conclusions

In conclusion, the ligature technique was used to produce an experimental periodontitis model that mimicked conditions of enhanced oxidative stress. To the best of our knowledge, the current study is the first to provide evidence indicating that LIPUS alleviates suppressed osteogenic differentiation and alveolar bone destruction due to periodontitis, by reducing oxidative stress. The Nrf2-mediated antioxidant defense mechanism, which plays an essential role in the protective effect against alveolar bone destruction, was upregulated and activated by LIPUS, and the PI3K/Akt-Nrf2 pathway played a partial role in this process. From a clinical point of view, these findings indicated that future studies of periodontal treatment modalities should pay more attention to the management of oxidative stress. LIPUS could be used as a physical therapy to promote periodontal regeneration after conventional treatment such as debridment and surface planning in periodontitis and diabetic periodontitis since oxidative stress was higher in diabetic periodontitis.

Abbreviations

3-NT: 3-nitrotyrosine; 4-HNE: 4-Hydroxy-nonenal; 8-OHdG: 8-Hydroxy-2′-deoxyguanosine; ALP: alkaline phosphatase; BV/TV: bone volume over total volume; CCK-8: cell Counting Kit-8; CEJ-ABC: cemento-enamel junction and alveolar bone crest; DAB: Diaminobenzidine; EDTA: ethylene diamine tetraacetic acid; FBS: fetal bovine serum; GAPDH: glyceraldehyde-3-phosphate dehydrogenase; HO-1: heme oxygenase-1; IL-6: interleukin-6; LIPUS: low intensity pulsed ultrasound; Micro-CT: Micro-computed tomography; MPO: myeloperoxidase; Nrf2: nuclear factor erythroid 2-related factor 2; OCN: osteocalcin; PBS: phosphate-buffered saline; PDLCs: periodontal ligament cells; PMSF: phenylmethanesulfonyl fluoride; RANKL: receptor activator for nuclear factor- κ B ligand; ROS: reactive oxygen species; Runx2: runt-related transcription factor-2; SD: Sprague-Dawley; SDS-PAGE: sodium dodecyl sulfate–polyacrylamide gel electrophoresis; siRNA-NC: siRNA-Negative control; Th.Tb: trabecular thickness; TNF-α: tumor necrosis factor-alpha; TRAP: tartrate-resistant acidic phosphatase.

Supplementary Material

Supplementary figures and tables.
http://www.thno.org/v10p9789s1.pdf

Acknowledgements

This work was supported by the National Natural Science Foundation of China (Grant No. 81771082 and 81700932) and the Natural Science Foundation of Chongqing (Grant No. cstc2017jcyjBX0019).

Author Contributions

Siqi Ying performed the experiments, analyzed the data and drafted the manuscript. Minmin Tan collected the data. Ge Feng proofread the article. Yunchun Kuang proofread the article. Duanjing Chen participated in discussions. Jie Li designed the study, guided the experiments and revised the manuscript. Jinlin Song provided financial support and final approval of manuscript.

Competing Interests

The authors have declared that no competing interest exists.

References

1. Eke PI, Wei L, Borgnakke WS, Thornton-Evans G, Zhang X, Lu H, et al. Periodontitis prevalence in adults >/= 65 years of age, in the USA. Periodontol 2000. 2016; 72: 76-95.
2. Page RC, Kornman KS. The pathogenesis of human periodontitis: an introduction. Periodontol 2000. 1997; 14: 9-11.
3. Saita M, Kaneko J, Sato T, Takahashi SS, Wada-Takahashi S, Kawamata R, et al. Novel antioxidative nanotherapeutics in a rat periodontitis model: Reactive oxygen species scavenging by redox injectable gel suppresses alveolar bone resorption. Biomaterials. 2016; 76: 292-301.
4. Ekuni D, Tomofuji T, Tamaki N, Sanbe T, Azuma T, Yamanaka R, et al. Mechanical stimulation of gingiva reduces plasma 8-OHdG level in rat periodontitis. Arch Oral Biol. 2008; 53: 324-9.
5. Gandhi KK, Pavaskar R, Cappetta EG, Drew HJ. Effectiveness of Adjunctive Use of Low-Level Laser Therapy and Photodynamic Therapy After Scaling and Root Planing in Patients with Chronic Periodontitis. Int J Periodontics Restorative Dent. 2019; 39: 837-43.
6. Lin Z, Meng L, Zou J, Zhou W, Huang X, Xue S, et al. Non-invasive ultrasonic neuromodulation of neuronal excitability for treatment of epilepsy. Theranostics. 2020; 10: 5514-26.
7. Xu T, Gu J, Li C, Guo X, Tu J, Zhang D, et al. Low-intensity pulsed ultrasound suppresses proliferation and promotes apoptosis via p38 MAPK signaling in rat visceral preadipocytes. Am J Transl Res. 2018; 10: 948-56.
8. Carina V, Costa V, Pagani S, De Luca A, Raimondi L, Bellavia D, et al. Inhibitory effects of low intensity pulsed ultrasound on osteoclastogenesis induced *in vitro* by breast cancer cells. J Exp Clin Cancer Res. 2018; 37: 197.
9. Erdogan O, Esen E. Biological aspects and clinical importance of ultrasound therapy in bone healing. J Ultrasound Med. 2009; 28: 765-76.
10. Fung CH, Cheung WH, Pounder NM, Harrison A, Leung KS. Osteocytes exposed to far field of therapeutic ultrasound promotes osteogenic cellular activities in pre-osteoblasts through soluble factors. Ultrasonics. 2014; 54: 1358-65.
11. Wang Y, Qiu Y, Li J, Zhao C, Song J. Low-intensity pulsed ultrasound promotes alveolar bone regeneration in a periodontal injury model. Ultrasonics. 2018; 90: 166-72.
12. Chen D, Xiang M, Gong Y, Xu L, Zhang T, He Y, et al. LIPUS promotes FOXO1 accumulation by downregulating miR-182 to enhance osteogenic differentiation in hPDLCs. Biochimie. 2019; 165: 219-28.
13. Miricescu D, Totan A, Calenic B, Mocanu B, Didilescu A, Mohora M, et al. Salivary biomarkers: relationship between oxidative stress and alveolar bone loss in chronic periodontitis. Acta Odontol Scand. 2014; 72: 42-7.
14. Muller G, Lubow C, Weindl G. Lysosomotropic beta blockers induce oxidative stress and IL23A production in Langerhans cells. Autophagy. 2019; p: 1-16.
15. Guo J, Li D, Tao H, Li G, Liu R, Dou Y, et al. Cyclodextrin-Derived Intrinsically Bioactive Nanoparticles for Treatment of Acute and Chronic Inflammatory Diseases. Adv Mater. 2019; 31: e1904607.
16. Ademowo OS, Sharma P, Cockwell P, Reis A, Chapple IL, Griffiths HR, et al. Distribution of plasma oxidised phosphatidylcholines in chronic kidney disease and periodontitis as a co-morbidity. Free Radic Biol Med. 2020; 146: 130-8.
17. Wu X, Chen X, Liu H, He ZW, Wang Z, Wei LJ, et al. Rescuing Dicer expression in inflamed colon tissues alleviates colitis and prevents colitis-associated tumorigenesis. Theranostics. 2020; 10: 5749-62.
18. Damgaard C, Kantarci A, Holmstrup P, Hasturk H, Nielsen CH, Van Dyke TE. Porphyromonas gingivalis-induced production of reactive oxygen species, tumor necrosis factor-alpha, interleukin-6, CXCL8 and CCL2 by neutrophils from localized aggressive periodontitis and healthy donors: modulating actions of red blood cells and resolvin E1. J Periodontal Res. 2017; 52: 246-54.
19. Chen M, Cai W, Zhao S, Shi L, Chen Y, Li X, et al. Oxidative stress-related biomarkers in saliva and gingival crevicular fluid associated with chronic periodontitis: A systematic review and meta-analysis. J Clin Periodontol. 2019; 46: 608-22.
20. Kuang Y, Hu B, Feng G, Xiang M, Deng Y, Tan M, et al. Metformin prevents against oxidative stress-induced senescence in human periodontal ligament cells. Biogerontology. 2020; 21: 13-27.
21. Kaspar JW, Niture SK, Jaiswal AK. Nrf2:INrf2 (Keap1) signaling in oxidative stress. Free Radic Biol Med. 2009; 47: 1304-9.
22. Hyeon S, Lee H, Yang Y, Jeong W. Nrf2 deficiency induces oxidative stress and promotes RANKL-induced osteoclast differentiation. Free Radic Biol Med. 2013; 65: 789-99.
23. Sima C, Aboodi GM, Lakschevitz FS, Sun C, Goldberg MB, Glogauer M. Nuclear Factor Erythroid 2-Related Factor 2 Down-Regulation in Oral Neutrophils Is Associated with Periodontal Oxidative Damage and Severe Chronic Periodontitis. Am J Pathol. 2016; 186: 1417-26.
24. Leewananthawet A, Arakawa S, Okano T, Daitoku Kinoshita R, Ashida H, Izumi Y, et al. Ozone ultrafine bubble water induces the cellular signaling involved in oxidative stress responses in human periodontal ligament fibroblasts. Sci Technol Adv Mater. 2019; 20: 589-98.
25. Li J, Li Y, Pan S, Zhang L, He L, Niu Y. Paeonol attenuates ligation-induced periodontitis in rats by inhibiting osteoclastogenesis via regulating Nrf2/NF-kappaB/NFATc1 signaling pathway. Biochimie. 2019; 156: 129-37.
26. Li J, Zhang Q, Ren C, Wu X, Zhang Y, Bai X, et al. Low-Intensity Pulsed Ultrasound Prevents the Oxidative Stress Induced Endothelial-Mesenchymal Transition in Human Aortic Endothelial Cells. Cell Physiol Biochem. 2018; 45: 1350-65.
27. Marchesan J, Girnary MS, Jing L, Miao MZ, Zhang S, Sun L, et al. An experimental murine model to study periodontitis. Nat Protoc. 2018; 13: 2247-67.
28. Graves DT, Fine D, Teng YT, Van Dyke TE, Hajishengallis G. The use of rodent models to investigate host-bacteria interactions related to periodontal diseases. J Clin Periodontol. 2008; 35: 89-105.
29. Zhou C, Liu C, Liu W, Chen W, Yin Y, Li CW, et al. SLFN11 inhibits hepatocellular carcinoma tumorigenesis and metastasis by targeting RPS4X via mTOR pathway. Theranostics. 2020; 10: 4627-43.
30. Boesing F, Patino JS, da Silva VR, Moreira EA. The interface between obesity and periodontitis with emphasis on oxidative stress and inflammatory response. Obes Rev. 2009; 10: 290-7.
31. Pirincciogluu AG, Gokalp D, Pirincciogluu M, Kizil G, Kizil M. Malondialdehyde (MDA) and protein carbonyl (PCO) levels as biomarkers of oxidative stress in subjects with familial hypercholesterolemia. Clin Biochem. 2010; 43: 1220-4.
32. Li X, Sun X, Zhang X, Mao Y, Ji Y, Shi L, et al. Enhanced Oxidative Damage and Nrf2 Downregulation Contribute to the Aggravation of Periodontitis by Diabetes Mellitus. Oxid Med Cell Longev. 2018; 2018: 9421019.
33. Huang CS, Lii CK, Lin AH, Yeh YW, Yao HT, Li CC, et al. Protection by chrysin, apigenin, and luteolin against oxidative stress is mediated by the Nrf2-dependent up-regulation of heme oxygenase 1 and glutamate cysteine ligase in rat primary hepatocytes. Arch Toxicol. 2013; 87: 167-78.
34. Zhang C, Li C, Chen S, Li Z, Jia X, Wang K, et al. Berberine protects against 6-OHDA-induced neurotoxicity in PC12 cells and zebrafish through hormetic mechanisms involving PI3K/AKT/Bcl-2 and Nrf2/HO-1 pathways. Redox Biol. 2017; 11: 1-11.
35. Zhuang S, Yu R, Zhong J, Liu P, Liu Z. Rhein from Rheum rhabarbarum Inhibits Hydrogen-Peroxide-Induced Oxidative Stress in Intestinal Epithelial Cells Partly through PI3K/Akt-Mediated Nrf2/HO-1 Pathways. J Agric Food Chem. 2019; 67: 2519-29.
36. Kuang Y, Hu B, Chen J, Feng G, Song J. Effects of periodontal endoscopy on the treatment of periodontitis: A systematic review and meta-analysis. J Am Dent Assoc. 2017; 148: 750-9.
37. Riccia DN, Bizzini F, Perilli MG, Polimeni A, Trinchieri V, Amicosante G, et al. Anti-inflammatory effects of Lactobacillus brevis (CD2) on periodontal disease. Oral Dis. 2007; 13: 376-85.
38. Oringer RJ, Research S, Therapy Committee of the American Academy of P. Modulation of the host response in periodontal therapy. J Periodontol. 2002; 73: 460-70.
39. Mirza YH, Teoh KH, Golding D, Wong JF, Nathdwarawala Y. Is there a role for low intensity pulsed ultrasound (LIPUS) in delayed or nonunion following arthrodesis in foot and ankle surgery? Foot Ankle Surg. 2019; 25: 842-8.
40. Cook SD, Salkeld SL, Patron LP, Doughty ES, Jones DG. The effect of low-intensity pulsed ultrasound on autologous osteochondral plugs in a canine model. Am J Sports Med. 2008; 36: 1733-41.
41. El-Mowafi H, Mohsen M. The effect of low-intensity pulsed ultrasound on callus maturation in tibial distraction osteogenesis. Int Orthop. 2005; 29: 121-4.
42. Zuo J, Zhen J, Wang F, Li Y, Zhou Z. Effect of Low-Intensity Pulsed Ultrasound on the Expression of Calcium Ion Transport-Related Proteins during Tertiary Dentin Formation. Ultrasound Med Biol. 2018; 44: 223-33.

43. Li JK, Chang WH, Lin JC, Ruaan RC, Liu HC, Sun JS. Cytokine release from osteoblasts in response to ultrasound stimulation. Biomaterials. 2003; 24: 2379-85.
44. Yue Y, Yang X, Wei X, Chen J, Fu N, Fu Y, et al. Osteogenic differentiation of adipose-derived stem cells prompted by low-intensity pulsed ultrasound. Cell Prolif. 2013; 46: 320-7.
45. Ahmadi-Motamayel F, Goodarzi MT, Jamshidi Z, Kebriaei R. Evaluation of Salivary and Serum Antioxidant and Oxidative Stress Statuses in Patients with Chronic Periodontitis: A Case-Control Study. Front Physiol. 2017; 8: 189.
46. Baser U, Gamsiz-Isik H, Cifcibasi E, Ademoglu E, Yalcin F. Plasma and salivary total antioxidant capacity in healthy controls compared with aggressive and chronic periodontitis patients. Saudi Med J. 2015; 36: 856-61.
47. Atabay VE, Lutfioglu M, Avci B, Sakallioglu EE, Aydogdu A. Obesity and oxidative stress in patients with different periodontal status: a case-control study. J Periodontal Res. 2017; 52: 51-60.
48. Li DJ, Zhao T, Xin RJ, Wang YY, Fei YB, Shen FM. Activation of alpha7 nicotinic acetylcholine receptor protects against oxidant stress damage through reducing vascular peroxidase-1 in a JNK signaling-dependent manner in endothelial cells. Cell Physiol Biochem. 2014; 33: 468-78.
49. Chen W, Zheng G, Yang S, Ping W, Fu X, Zhang N, et al. CYP2J2 and EETs Protect against Oxidative Stress and Apoptosis *in Vivo* and *in Vitro* Following Lung Ischemia/Reperfusion. Cell Physiol Biochem. 2014; 33: 1663-80.
50. Wang M, Kanako N, Zhang Y, Xiao X, Gao Q, Tetsuya K. A unique polysaccharide purified from Hericium erinaceus mycelium prevents oxidative stress induced by H2O2 in human gastric mucosa epithelium cell. PLoS One. 2017; 12: e0181546.
51. Tomofuji T, Ekuni D, Sanbe T, Irie K, Azuma T, Maruyama T, et al. Effects of vitamin C intake on gingival oxidative stress in rat periodontitis. Free Radic Biol Med. 2009; 46: 163-8.
52. Borges I, Jr., Moreira EA, Filho DW, de Oliveira TB, da Silva MB, Frode TS. Proinflammatory and oxidative stress markers in patients with periodontal disease. Mediators Inflamm. 2007; 2007: 45794.
53. Sculley DV, Langley-Evans SC. Salivary antioxidants and periodontal disease status. Proc Nutr Soc. 2002; 61: 137-43.
54. Wauquier F, Leotoing L, Coxam V, Guicheux J, Wittrant Y. Oxidative stress in bone remodelling and disease. Trends Mol Med. 2009; 15: 468-77.
55. Hawkins CL, Morgan PE, Davies MJ. Quantification of protein modification by oxidants. Free Radic Biol Med. 2009; 46: 965-88.
56. Obrosova IG, Drel VR, Oltman CL, Mashtalir N, Tibrewala J, Groves JT, et al. Role of nitrosative stress in early neuropathy and vascular dysfunction in streptozotocin-diabetic rats. Am J Physiol Endocrinol Metab. 2007; 293: E1645-55.
57. Kasai H. Chemistry-based studies on oxidative DNA damage: formation, repair, and mutagenesis. Free Radic Biol Med. 2002; 33: 450-6.
58. Luo X, Zhang H, Duan Y, Chen G. Protective effects of radish (Raphanus sativus L.) leaves extract against hydrogen peroxide-induced oxidative damage in human fetal lung fibroblast (MRC-5) cells. Biomed Pharmacother. 2018; 103: 406-14.
59. Morabito R, Remigante A, Di Pietro ML, Giannetto A, La Spada G, Marino A. SO4(=) uptake and catalase role in preconditioning after H2O2-induced oxidative stress in human erythrocytes. Pflugers Arch. 2017; 469: 235-50.
60. Chen WC, Hsieh SR, Chiu CH, Hsu BD, Liou YM. Molecular identification for epigallocatechin-3-gallate-mediated antioxidant intervention on the H2O2-induced oxidative stress in H9c2 rat cardiomyoblasts. J Biomed Sci. 2014; 21: 56.
61. Chisci E, De Giorgi M, Zanfrini E, Testasecca A, Brambilla E, Cinti A, et al. Simultaneous overexpression of human E5NT and ENTPD1 protects porcine endothelial cells against H2O2-induced oxidative stress and cytotoxicity *in vitro*. Free Radic Biol Med. 2017; 108: 320-33.
62. Darveau RP. Periodontitis: a polymicrobial disruption of host homeostasis. Nat Rev Microbiol. 2010; 8: 481-90.
63. Albandar JM. Aggressive and acute periodontal diseases. Periodontol 2000. 2014; 65: 7-12.
64. Wang L, Zhang YG, Wang XM, Ma LF, Zhang YM. Naringin protects human adipose-derived mesenchymal stem cells against hydrogen peroxide-induced inhibition of osteogenic differentiation. Chem Biol Interact. 2015; 242: 255-61.
65. Barrera G, Pizzimenti S, Ciamporcero ES, Daga M, Ullio C, Arcaro A, et al. Role of 4-hydroxynonenal-protein adducts in human diseases. Antioxid Redox Signal. 2015; 22: 1681-702.
66. Nguyen T, Nioi P, Pickett CB. The Nrf2-antioxidant response element signaling pathway and its activation by oxidative stress. J Biol Chem. 2009; 284: 13291-5.
67. Niture SK, Khatri R, Jaiswal AK. Regulation of Nrf2-an update. Free Radic Biol Med. 2014; 66: 36-44.
68. Pan H, Guan D, Liu X, Li J, Wang L, Wu J, et al. SIRT6 safeguards human mesenchymal stem cells from oxidative stress by coactivating NRF2. Cell Res. 2016; 26: 190-205.
69. Liu Q, Gao Y, Ci X. Role of Nrf2 and Its Activators in Respiratory Diseases. Oxid Med Cell Longev. 2019; 2019: 7090534.
70. Silva-Islas CA, Maldonado PD. Canonical and non-canonical mechanisms of Nrf2 activation. Pharmacol Res. 2018; 134: 92-9.
71. Liu Y, Yang H, Wen Y, Li B, Zhao Y, Xing J, et al. Nrf2 Inhibits Periodontal Ligament Stem Cell Apoptosis under Excessive Oxidative Stress. Int J Mol Sci. 2017; 18.
72. Bryan HK, Olayanju A, Goldring CE, Park BK. The Nrf2 cell defence pathway: Keap1-dependent and -independent mechanisms of regulation. Biochem Pharmacol. 2013; 85: 705-17.
73. Xie S, Jiang X, Wang R, Xie S, Hua Y, Zhou S, et al. Low-intensity pulsed ultrasound promotes the proliferation of human bone mesenchymal stem cells by activating PI3K/AKt signaling pathways. J Cell Biochem. 2019; 120: 15823-33.